Supporting Information

Fully water-soluble, High-Performance Transient Sensors on a Versatile Galactomannan Substrate Derived from the Endosperm

Ning Yi, Zheng Cheng, Lei Yang, Gregory Edelman, Cuili Xue, Yi Ma, Hongli Zhu, Huanyu Cheng**

N. Yi, H. Cheng
Department of Materials Science and Engineering
The Pennsylvania State University
University Park, Pennsylvania 16802, USA
E-mail: huanyu.cheng@psu.edu

Z. Cheng, L. Yang, Y. Ma, H. Zhu
Department of Mechanical and Industrial Engineering
Northeastern University
Boston, Massachusetts 02115, USA

G. Edelman, C. Xue, H. Cheng
Department of Engineering Science and Mechanics
Materials Research Institute
The Pennsylvania State University
University Park, Pennsylvania 16802, USA

C. Xue
School of Precision Instrument and Optoelectronics Engineering
Tianjin University
Tianjin, 300072, China

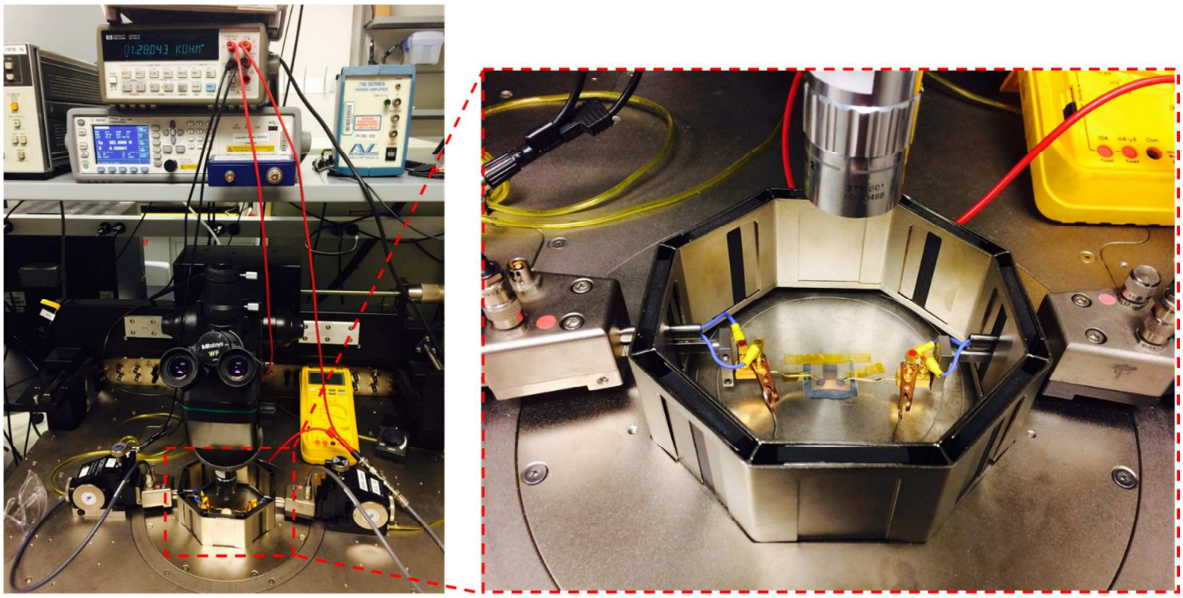

Figure S1 | Experimental setup for the calibration of the temperature sensor. The temperature sensor is fixed on a probe station and connected to a digital multimeter. A magnified view of the sample on the probe station is shown in the inset.

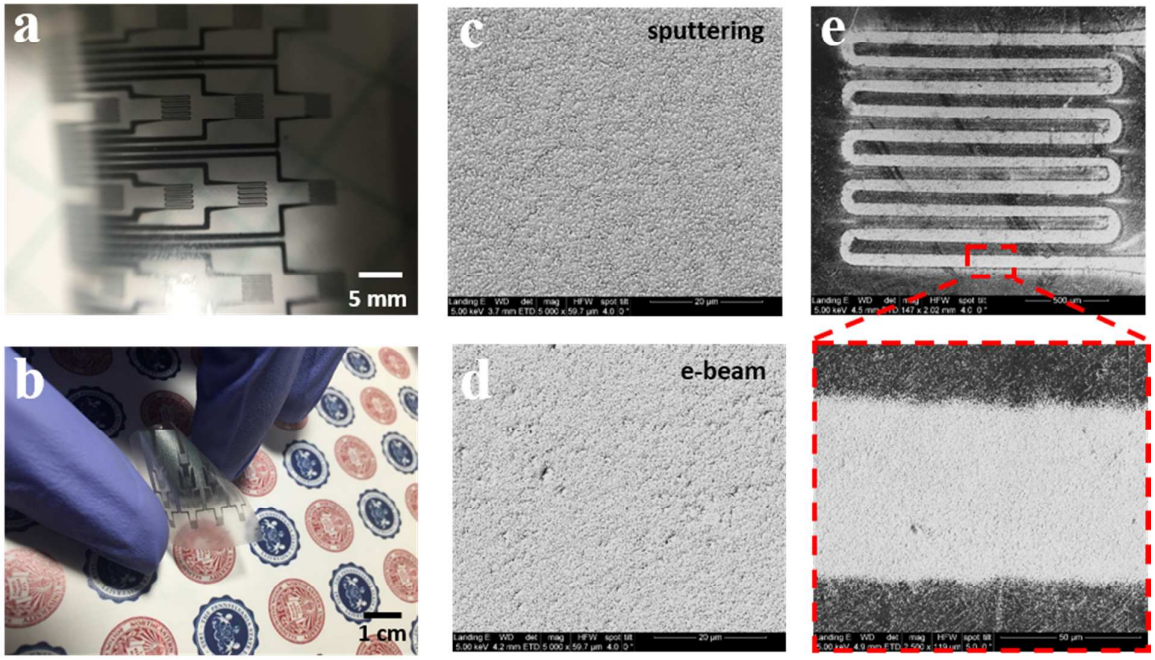

Figure S2 | (a) Optical image of the temperature sensor array. **(b)** Bending of the temperature sensor array. Photo credit: H. Cheng, Penn State University® and Northeastern University®. **(c)** SEM image of sputtered zinc thin layer on a galactomannan film. **(d)** SEM image of e-beam evaporated zinc thin layer on a galactomannan film. **(e)** SEM image of an individual temperature sensor fabricated via e-beam evaporation. The inset shows the magnified view of the zinc traces.

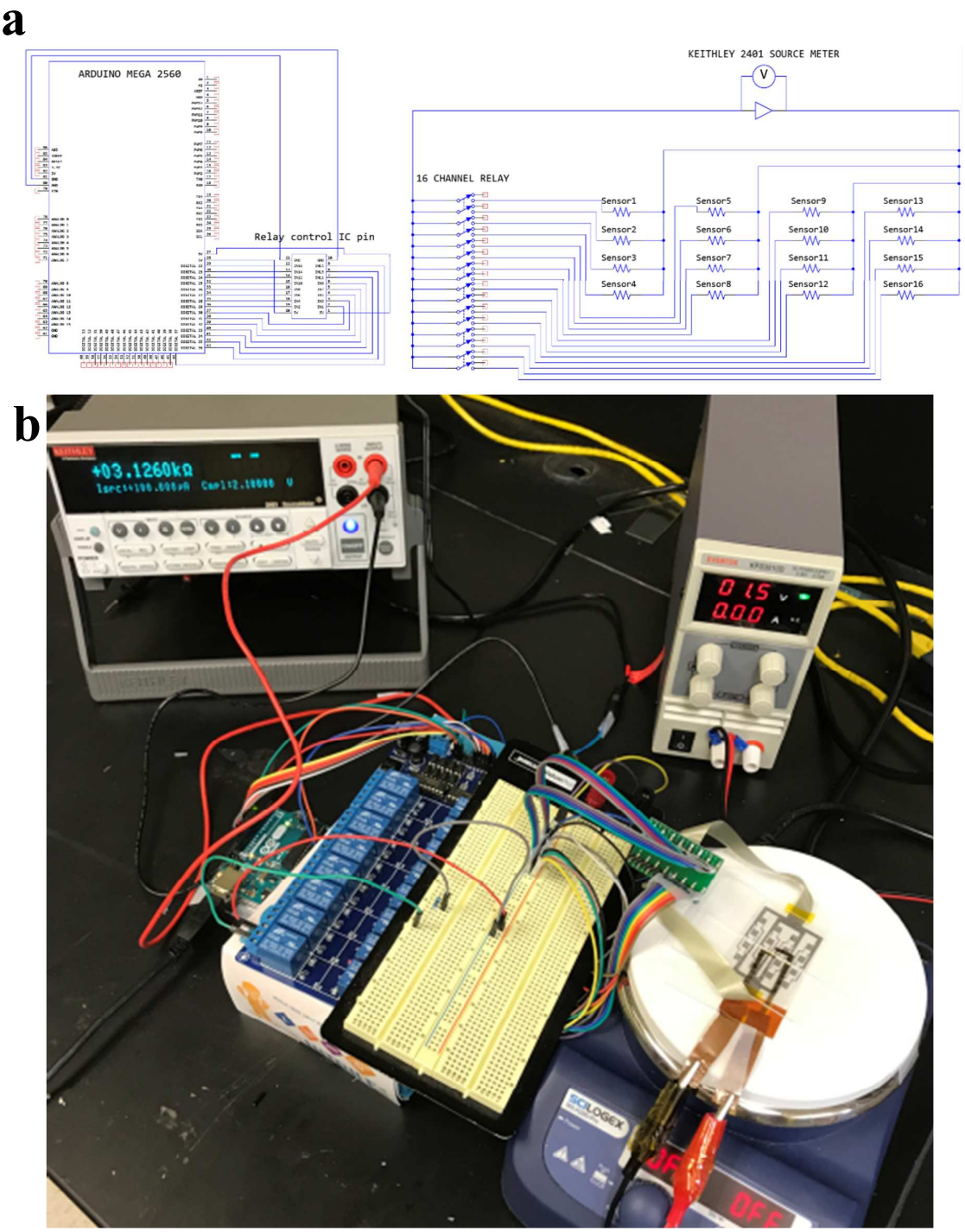

Figure S3 | (a) Circuit diagrams of the four by four temperature sensor array and the multiplexing circuit. **(b)** Photo of the experimental setup of the multiplexing circuit with a voltage source and a heater.

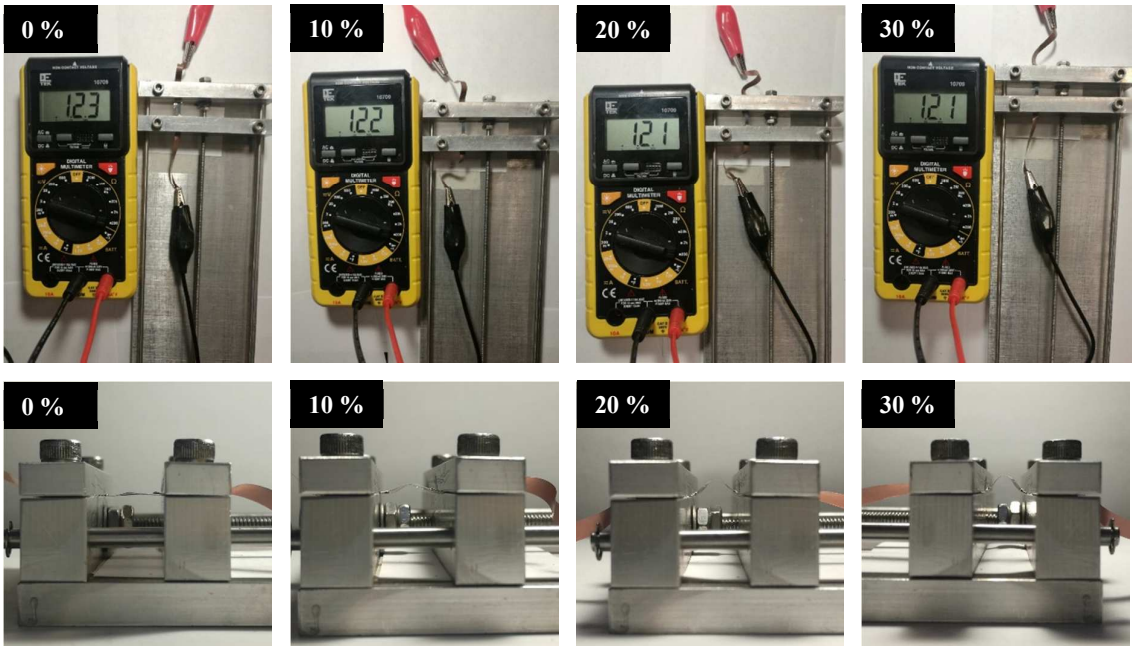

Figure S4 | Resistance measurement from the Zn electrode subject to a compressive strain (0-30 %) that induces bending with different radii of curvature. Negligible resistance change (< 2 %) was observed upon bending.

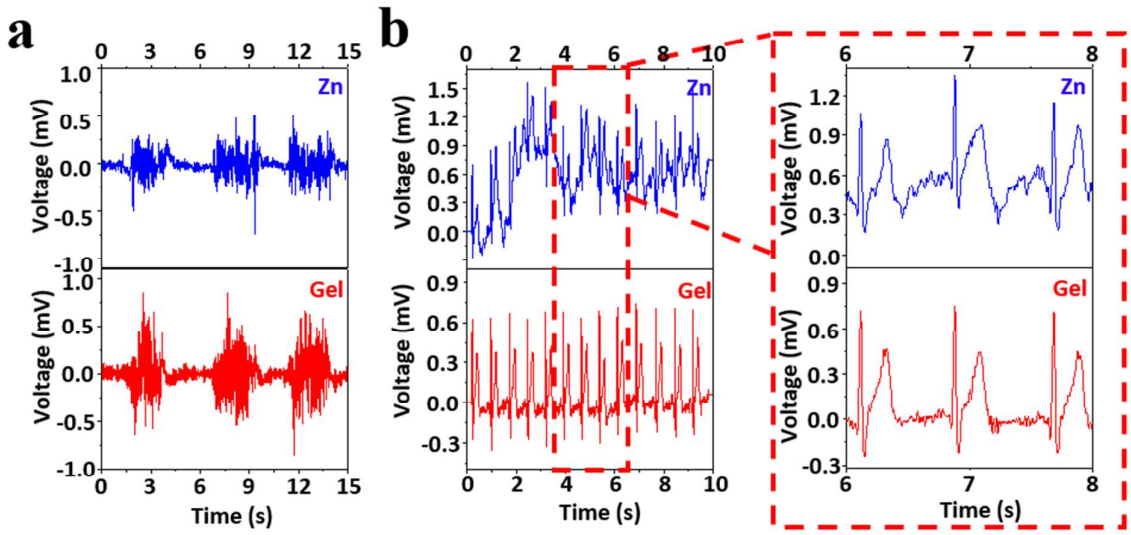

Figure S5 | (a) EMG signals measured from the Zn and Gel electrodes after storage of the zinc electrodes for 15 days. **(b)** ECG signals measured from the Zn and Gel electrodes after storage of the zinc electrodes for 15 days. The baseline drift of the ECG signal is more evident compared with the signals collected from the newly fabricated electrodes. A magnified view of the signal is shown in the inset.

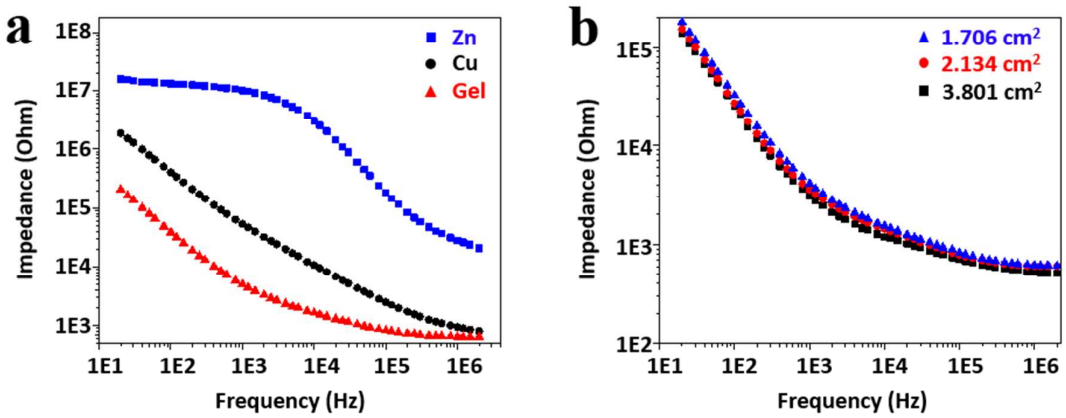

Figure S6 | (a) Impedance between the skin surface and the Zn (or Cu) electrodes, measured after 15 days of their fabrication. The results were compared to that measured from the commercial gel electrode. **(b)** Contact impedance as a function of frequency from the commercial gel electrode with different sizes. Smaller electrode size yielded a higher impedance value.

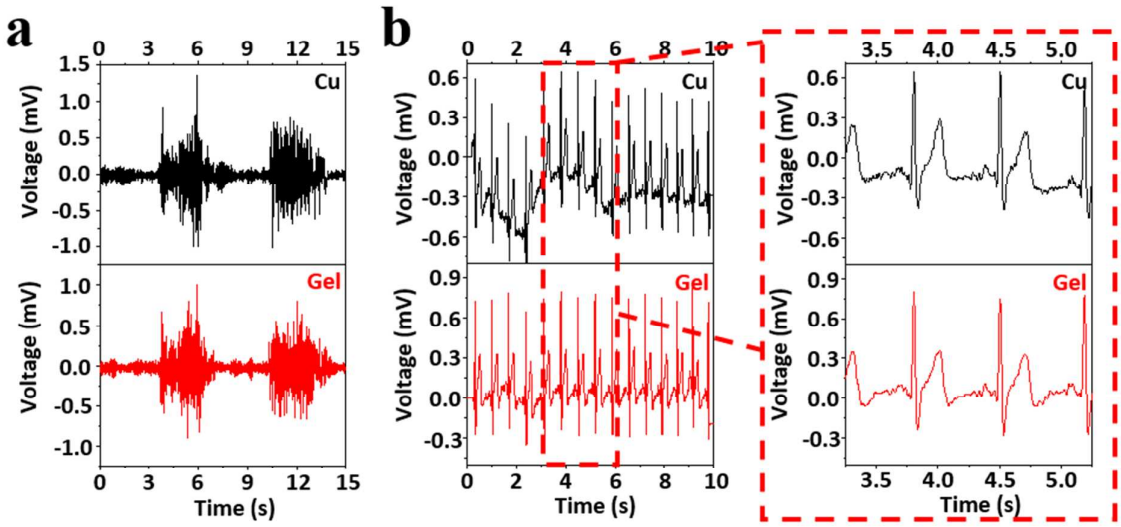

Figure S7 | (a) EMG signals measured from the Cu and Gel electrodes. **(b)** ECG signals measured from the Cu and Gel electrodes. Baseline drift of the ECG signal is more obvious in the signal measured from the Cu electrode than that from the gel electrode. A magnified view of the signal is shown in the inset.

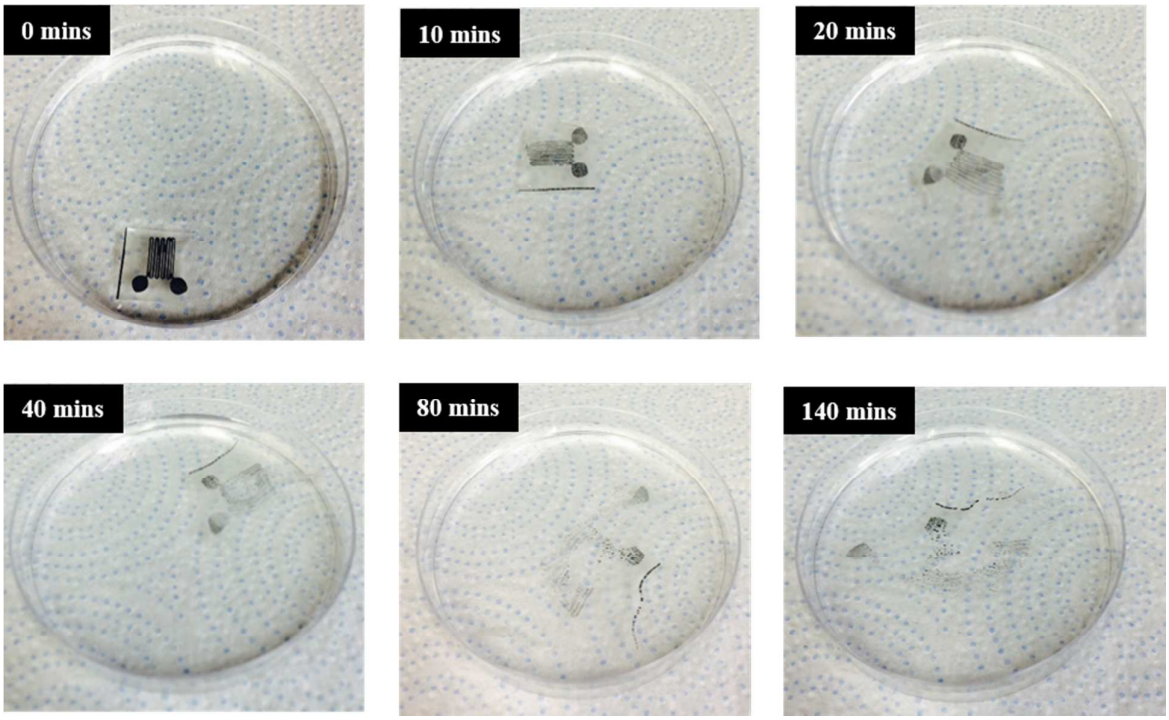

Figure S8 | Dissolution of the temperature sensor after being placed on the water surface for 0 minutes, 10 minutes, 20 minutes, 40 minutes, 80 minutes, and 140 minutes.

Figure S9 | Dissolution of the Zn electrode (taped to the petri dish) after being immersed in water for 0 hours, 12 hours, and 24 hours. Photo credit: H. Cheng, Penn State University® and Northeastern University®.